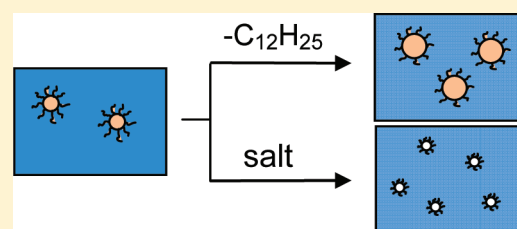


# Effects of Hydrophobic Substituents and Salt on Core–Shell Aggregates of Hydrophobically Modified Chitosan: Light Scattering Study

Evgeniya V. Korchagina and Olga E. Philippova\*

Physics Department, Moscow State University, Moscow 119991, Russia

**ABSTRACT:** In this study we examine two methods of enhancement of aggregation of hydrophobically modified chitosan in dilute aqueous solutions: by increasing the content of *n*-dodecyl substituents, favoring hydrophobic association, and by increasing the amount of added low molecular weight salt, screening the electrostatic repulsion between similarly charged aggregating chains. By static and dynamic light scattering it was demonstrated that at the growth of the content of hydrophobic groups in the polymer (2–4 mol %) and of the amount of salt in solution (0.025–0.1 M) the weight fraction of aggregates increases, but the aggregation number remains unchanged. This behavior was attributed to the core–shell structure of the aggregates, which provides a low surface energy and strong attraction of associating groups inside the core. At the same time, the effects of the content of hydrophobic groups in the polymer and the ionic strength of the solution on the radii of the aggregates are quite different. Increasing the content of hydrophobic groups induces growth of the gyration radii of the aggregates, but does not affect their hydrodynamic radii. These data suggest the expansion of the hydrophobic core of the aggregates and the contraction of their highly swollen shell. On the other hand, increasing the salt concentration leads to a decrease of both the gyration and hydrodynamic radii of the aggregates, which is due to partial screening of electrostatic repulsion between similarly charged units and lowering of the osmotic pressure of counterions confined inside the aggregates.



## INTRODUCTION

Chitosan is a linear polysaccharide consisting of  $\beta(1\rightarrow4)$ -linked 2-amino-2-deoxy-D-glucose (GlcN) and *N*-acetyl-2-amino-2-deoxy-D-glucose (GlcNAc) residues. It occurs naturally in some fungi (Mucoraceae),<sup>1</sup> but mainly it is produced by alkali *N*-deacetylation of chitin, the second most abundant polysaccharide on the earth after cellulose.<sup>2</sup>

Chitosan is a nontoxic, biocompatible, and biodegradable polymer.<sup>1–3</sup> Also, it possesses various bioactivities, including hemostatic, hypolipidemic, immunoadjuvant, and antimicrobial activity.<sup>3</sup> Due to its unique combination of properties, chitosan has found numerous applications in the pharmacy, biotechnology, food, cosmetics, etc., industries.<sup>1–3</sup>

Chitosan is soluble in water at acidic pH, when most of the amino groups are protonated, but even fully protonated chitosan tends to form aggregates<sup>4–14</sup> in dilute aqueous solutions due to hydrogen bonding and hydrophobic interactions. The aggregates represent nanogels with a denser core and highly swollen shell.<sup>11</sup> It was suggested that within the aggregates different polymer chains are linked together by junction zones formed either by microblocks of GlcNAc units<sup>5,13</sup> or by stereoregular sequences of GlcN units.<sup>14</sup> In the latter case crystallization of the junction zones may occur.<sup>14–16</sup> Most probably the junction zones consist of parallel arranged fragments of different chains, which facilitates a cooperative formation of multiple hydrogen bonds and hydrophobic links between them.

The tendency to aggregate can be enhanced if some hydrophobic side groups are introduced in chitosan chains. If the initial chitosan was prone to aggregation, within the aggregates (nanogels) of hydrophobically modified (HM) chitosan two types of cross-links between polymer chains will be formed:<sup>8</sup> (1) those inherent to chitosan itself and (2) micelle-like domains typical for many water-soluble polymers with attracting hydrophobic side groups.

The aggregates of HM chitosan are very promising as carriers for drug delivery due to the unique properties of chitosan combined with the presence of hydrophobic moieties, which create a depot for storage of drugs poorly soluble in water. The understanding of the impact of the content of hydrophobic substituents on the size and the aggregation number of the nanogels is quite important for designing drug-carrying vehicles. Also, it is crucial to gain insight into the effect of salt on the properties of nanogels as salt is present in many biological liquids.

Theoretical considerations show<sup>17,18</sup> that the aggregates formed by HM polyelectrolytes should have some optimum size determined by the competition between attraction of associating groups, inducing growth of aggregates, and electrostatic repulsion, limiting their growth. Following these considerations, the enhancement of aggregation by increasing

Received: April 1, 2012

Revised: May 1, 2012

Published: May 1, 2012

the content of associating groups or by adding salt, which reduces the repulsion between the chains, should lead to the formation of aggregates of larger size. Despite rather obvious tendencies predicted theoretically, the experimental data on HM chitosan samples are rather contradictory. In particular, it was observed that in some cases the hydrodynamic radius of aggregates,  $R_{h,agg}$ , increases with increasing amount of hydrophobic groups;<sup>19</sup> in other cases it decreases.<sup>20–25</sup> The effect of salt on the  $R_{h,agg}$  values of HM chitosan is also ambiguous as salt can induce either compactization<sup>20,26</sup> or growth<sup>27,28</sup> of the aggregates. The influence of hydrophobes and salt on other important characteristics of aggregates such as their aggregation number still remains unstudied.

Therefore, the aim of the present work is to investigate the effect of the content of hydrophobic groups and of the amount of added salt on the size and the aggregation number of multichain aggregates of HM chitosan formed in dilute aqueous acidic solutions. The knowledge of these regularities is crucial for the design of drug delivery systems based on HM chitosan.

## EXPERIMENTAL SECTION

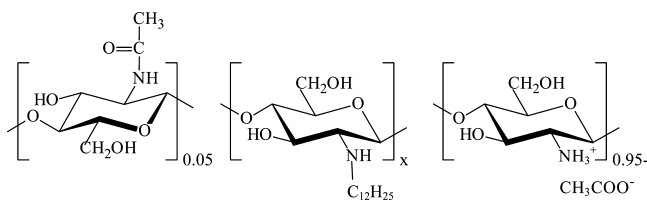
**Materials.** Acetic acid (99.8%) from Fluka and sodium chloride (99.5%) and ammonium acetate (99.5%) from Helicon were used without additional purification. Pyrene from Aldrich was recrystallized three times from ethanol. For the preparation of solutions, deionized distilled water from a Milli-Q system (Millipore) was used.

Chitosan was obtained by alkaline N-deacetylation of chitin from Far East crab shells and purified from metal salts by repeated precipitation from 1 M HCl solution to 2 M NaOH and washing of the precipitate by distilled water.<sup>29</sup>

Chitosan with  $M_w = 75\,000$  (degree of polymerization 460) was obtained by acid hydrolysis of the purified high molecular weight chitosan sample in homogeneous medium followed by fractional precipitation. According to NMR data, the prepared polymer contains 5 mol % GlcNAc repeat units randomly distributed along the chains.

HM chitosans (Chart 1) were prepared by reductive amination of chitosan in homogeneous conditions using *n*-dodecanaldehyde as

Chart 1. Chemical Structure of HM Chitosan under Study<sup>a</sup>



<sup>a</sup>The fraction of hydrophobic units  $x$  is equal to 0.02 or 0.04.

described elsewhere.<sup>30</sup> The reaction does not affect the molecular weight of the polymer. The content of hydrophobic *N*-dodecyl-D-glucosamine units, i.e., the degree of substitution (DS), was determined by <sup>1</sup>H NMR analysis.<sup>30</sup> It was found to be equal to 2 and 4 mol % for the two HM chitosan samples prepared. These samples are further designated as HMC-2% and HMC-4%, respectively. It should be noted that a larger amount of *n*-dodecyl groups cannot be incorporated into the chitosan samples under study without loss of their solubility in aqueous acid solutions.

**Sample Preparation.** CH<sub>3</sub>COOH (0.3 M) with different amounts of added NaCl was used as a solvent for both the preparation of polymer solutions and all dilutions. Prior to use, it was filtered through a 0.22 μm Millipore Millex-LCR filter. Stock solutions of HM chitosans with concentrations of ca. 1.0–1.5 g/L were prepared by slow dropwise addition of the solvent to polymer powder. The mixture was homogenized by stirring for at least 2 days at room temperature. Solutions with other concentrations of polymer were prepared by

appropriate dilution of the stock solution. Before all measurements the polymer solutions were filtered through a 0.45 μm Millipore Millex-LCR filter to remove the dust. To evaluate the loss of polymer after filtration, the reaction of ninhydrin with a primary amino group,<sup>31–33</sup> leading to the formation of a color reaction product (Ruhemann's purple), was used.

All experiments were performed with dilute solutions of chitosan and HM chitosan. The amount of acetic acid (0.3 M) was sufficient to fully charge all amino groups of the polymers.<sup>34</sup> At these conditions the mean distance between the charged units in the macromolecules of chitosan is ca. 5.5 Å.<sup>11</sup>

In dilute polyelectrolyte solutions the electrostatic interactions are screened at length scales larger than the Debye length,  $r_D$ . The values of  $r_D$  in the solutions under study were estimated with the formula<sup>35</sup>

$$r_D = \sqrt{\epsilon_0 \epsilon k_B T / 4\pi e^2 \left( \frac{1}{2} \sum c_i z_i^2 \right)} \quad (1)$$

where  $\epsilon$  is the dielectric constant,  $k_B$  is the Boltzmann constant,  $T$  is the absolute temperature,  $e$  is the elementary charge,  $(1/2) \sum c_i z_i^2$  is the ionic strength of the solution, and  $c_i$  and  $z_i$  are the concentration and the valence of ions of a given type. When the ionic strength was calculated, only the contribution of sodium chloride was taken into account while the input of dissociated acetic acid was neglected because it is quite small. The  $r_D$  values obtained are summarized in Table 1.

Table 1. Debye Lengths,  $r_D$ , in NaCl Solutions of Different Concentrations and Their Ratios,  $r_D/l$ , with the Average Distance between Charged Units in Fully Charged Chitosan Chains

[NaCl], M	$r_D$ , Å	$r_D/l$
0.025	19	3.6
0.05	13.6	2.6
0.1	9.7	1.8

**Light Scattering Measurements.** Static light scattering (SLS) and dynamic light scattering (DLS) measurements were performed on an ALV/DLS/SLS-5000 compact goniometer system equipped with an ALV digital time correlator, computer-controlled and stepping-motor-driven variable-angle detection system, and a thermostat with temperature stabilization of 0.1 °C. All measurements were made at 25 °C. The excitation source was a helium–neon vertically polarized laser operating at a wavelength of 632.8 nm.

SLS experiments were carried out for determining the second virial coefficient,  $A_2$ , the apparent weight-average molecular weight,  $M_w^*$ , and the apparent *z*-average radius of gyration,  $R_g^*$ . In SLS experiments the absolute scattered intensity,  $R_\theta(q)$  (excess Rayleigh ratio), of the solute particles is determined from the experimentally measured scattered intensities of the solution,  $I_{\text{solution}}$ , and of the solvent,  $I_{\text{solvent}}$ , as well as the intensity measured for a toluene sample standard,  $I_{\text{toluene}}$ , renormalized by the so-called absolute scattering intensity of the standard  $I_{\text{toluene,abs}}$ :<sup>36</sup>

$$R_\theta(q) = (I_{\text{solution}} - I_{\text{solvent}}) \frac{I_{\text{toluene,abs}}}{I_{\text{toluene}}} \quad (2)$$

The SLS experiments were carried out at scattering angles ranging from 30° to 150°.

To account for the effects of the particle concentration, the particle form factor, and solute–solvent interactions on the measured scattering intensity, the Zimm expression<sup>37</sup> was used:

$$\frac{Kc}{R_\theta(q)} \approx \frac{1}{M_w} \left( 1 + \frac{1}{3} R_g^2 q^2 \right) + 2A_2c \quad (3)$$

where  $c$  is the polymer concentration,  $K = 4\pi^2 n^2 (dn/dc)^2 / N_A \lambda^4$  is the scattering constant, and  $q = (4\pi/\lambda) \sin(\theta/2)$  is the scattering vector. Here  $N_A$  is Avogadro's number,  $\lambda$  is the wavelength of light in a

vacuum,  $n$  is the refractive index of the solvent, and  $dn/dc$  is the refractive index increment. According to eq 3, the extrapolation  $(Kc/R_\theta)_{c \rightarrow 0, q \rightarrow 0}$  gives the  $1/M_w$  value, whereas the slopes of  $(Kc/R_\theta)_{c \rightarrow 0}$  vs  $q^2$  and  $(Kc/R_\theta)_{q \rightarrow 0}$  vs  $c$  lead to  $R_g$  and  $A_2$  values, respectively.

DLS measurements were carried out for determining the hydrodynamic radii,  $R_H$ , of scattering particles. The scattering angle  $\theta$  was varied between  $30^\circ$  and  $90^\circ$ . In DLS experiments the normalized time autocorrelation function,  $g^{(2)}(q, t)$ , of the scattered intensity is measured and expressed in terms of the field autocorrelation function,  $g^{(1)}(q, t)$  (or the autocorrelation function of the concentration fluctuations), through the equation<sup>36</sup>

$$g^{(2)}(q, t) = \frac{\langle I(q, t)I(q, 0) \rangle}{\langle I(q, 0) \rangle^2} = A + \beta |g^{(1)}(q, t)|^2 \quad (4)$$

where  $I(q, 0)$  and  $I(q, t)$  are the scattering intensities at time  $t = 0$  and at a certain delay time  $t$  later,  $A$  is the baseline, and  $\beta$  is the coherence factor.

The distribution of decay rates (reciprocal relaxation times),  $G(\Gamma)$ , was determined from the correlation function  $g^{(1)}(q, t)$  using the CONTIN algorithm.<sup>38</sup> It is based on the Laplace inversion of the  $g^{(1)}(q, t)$  function.<sup>38</sup> When the spectral profile of the scattered light can be described by a multi-Lorentzian curve,  $g^{(1)}(q, t)$  can be written as

$$g^{(1)}(q, t) = \int_0^\infty G(\Gamma) \exp(-\Gamma t) d\Gamma \quad (5)$$

In the case of a diffusive process,  $\Gamma$  is related to the translational diffusion coefficient,  $D$ , by  $D = (\Gamma/q^2)|_{q=0, c=0}$ , so that  $G(\Gamma)$  can be converted into a translational diffusion coefficient distribution or a hydrodynamic radius distribution by using the Einstein–Stokes equation:<sup>36</sup>

$$R_H = \frac{k_B T}{6\pi D \eta_s} \quad (6)$$

where  $\eta_s$  is the solvent viscosity.

The gyration radii of the aggregates,  $R_{g,agg}$ , were obtained from the scattering intensity provided by the slow mode according to the following relation:

$$P(q) = 1 - \frac{1}{3} R_{g,agg}^2 q^2 \quad (7)$$

where  $P(q)$  is the particle scattering factor, which represents the ratio of the scattering light intensity at wave vector  $q$  to the zero-wave-vector scattering light intensity.

The polymer volume fraction,  $\phi_{agg}$ , in the aggregates was estimated by the following formula under the assumption that the aggregates can be regarded as homogeneous spheres:

$$\phi_{agg} = \frac{\bar{v} M_{agg}}{N_A (4\pi/3) R_{g,agg}^3} \quad (8)$$

where  $\bar{v}$  is the specific volume of chitosan equal to 0.57 mL/g,  $M_{agg}$  is the molecular weight of the aggregates, and  $R_{g,agg}$  is their gyration radius.

**Refractive Index Increment Determination.** Refractive index increment,  $dn/dc$ , values of chitosan and HM chitosan solutions were measured with an Optilab refractometer (Wyatt Technology) operating at a wavelength of 632.8 nm at 25 °C. Six concentrations of dilute polymer solutions were analyzed for each determination of the  $dn/dc$  value. The solutions were prepared by independent dilution of a stock 1.5 g/L solution of polymer in 0.3 M CH<sub>3</sub>COOH in the presence of different concentrations of NaCl. Before measurements all solutions and solvents were degassed to remove air bubbles. Despite the presence of aggregates in all solutions of chitosan and HM chitosan, the plots of refractive index versus polymer concentration represent straight lines passing through the origin; from the slopes of these plots the  $dn/dc$  values were determined. The results are summarized in Table 2. It is seen that the values of  $dn/dc$  are independent of the content of hydrophobic groups and decrease with increasing salt concentration.

**Table 2. Refractive Index Increments of HM Chitosan Solutions in 0.3 M CH<sub>3</sub>COOH at Different Concentrations of NaCl**

[NaCl], M	DS, mol %	$dn/dc$ , mL/g
0.025	0	0.200 ± 0.005
	2	0.200 ± 0.005
	4	0.200 ± 0.005
0.05	0	0.195 ± 0.005
	2	0.195 ± 0.005
	4	0.195 ± 0.005
0.1	0	0.190 ± 0.005
	2	0.190 ± 0.005
	4	0.190 ± 0.005

**Viscosity Measurements.** Viscosity measurements were performed with a standard Ubbelohde viscometer at 25.0 ± 0.1 °C. Each measurement was repeated at least three times. All the investigated samples show linear dependences of the reduced viscosity,  $\eta_{red}$ , on the polymer concentration,  $c$ . From these dependences the Huggins constants,  $k_H$ , were estimated according to the equation<sup>39</sup>

$$\eta_{red} = [\eta] + k_H c [\eta]^2 \quad (9)$$

where  $[\eta]$  is the intrinsic viscosity of the solution.

**UV Spectroscopy Measurements.** UV spectra of pyrene solutions were recorded with a Hewlett–Packard 8452A photodiode array spectrometer using a 1 cm path length quartz cuvette. For analysis of the data an absorbance at 338 nm with respect to the baseline was used. At pyrene concentrations below the limiting solubility, the optical density at 338 nm is linearly proportional to the concentration of added pyrene. As soon as saturation of the polymer solution by pyrene is achieved, the measured optical density levels off.<sup>40</sup>

Solutions for the measurements of UV spectra were prepared as follows. Equal aliquots (0.02 mL) of stock solutions of pyrene in ethanol with different concentrations were added to 2 mL of 1 g/L aqueous polymer solutions. The concentration of added pyrene was varied from  $1.0 \times 10^{-6}$  to  $4.0 \times 10^{-5}$  mol/L. The resulting solutions were left for 3 days at room temperature for equilibration prior to the measurements.

## RESULTS AND DISCUSSION

**Effect of the Content of Hydrophobic Groups.** First the effect of polymer hydrophobicity on the viscosity of HM chitosan solutions was investigated. The data obtained are presented in Table 3. It is seen that the Huggins constants,  $k_H$ ,

**Table 3. Viscosity of HM Chitosan Solutions in 0.3 M CH<sub>3</sub>COOH at Different Concentrations of NaCl**

[NaCl], M	DS, mol %	$[\eta]$ , mL/g	$C^*$ , <sup>a</sup> g/L	$k_H$
0.025	2	650	1.5	0.42
	4	650	1.5	0.60
0.05	2	500	2.0	0.45
	4	500	2.0	0.74
0.1	2	480	2.1	0.50
	4	480	2.1	0.97

<sup>a</sup>The overlap concentration was estimated as  $C^* = 1/[\eta]$ .

increase with increasing content of hydrophobic units, thus pointing to stronger interpolymer interactions. At the same time, the intrinsic viscosity,  $[\eta]$ , does not depend on the polymer hydrophobicity, which indicates the absence of intramolecular aggregation. Most probably, this is due to the semirigid character of the chitosan backbone<sup>2</sup> and a small

number of hydrophobic substituents in a single chain. Indeed, simple calculations show that spherical micelle-like domains with radius equal to the contour length of the *n*-dodecyl group (15.4 Å) should contain ca. 40 *n*-dodecyl groups to avoid their unfavorable contact with water. In the polymers under study the content of hydrophobic groups per chain is much smaller (it equals ca. 9 for HMC-2% and ca. 18 for HMC-4%), which makes the intramolecular aggregation of hydrophobes unfavorable. Thus, viscosity data suggest that HM chitosan forms intermolecular aggregates in dilute solutions.

The aggregation was further investigated by DLS. For all chitosan samples under study, independently of their hydrophobicity, the correlation functions  $g^{(1)}(q,t)$  of polymer concentration fluctuations show a bimodal relaxation behavior with fast and slow relaxation modes (Figure 1):

$$g^{(1)}(q, t) = A_{\text{fast}} \exp\left(-\frac{t}{\tau_{\text{fast}}}\right) + A_{\text{slow}} \exp\left(-\frac{t}{\tau_{\text{slow}}}\right) \quad (10)$$

Here  $\tau_{\text{fast}}$  and  $\tau_{\text{slow}}$  are the fast and slow relaxation times, respectively, and  $A_{\text{fast}}$  and  $A_{\text{slow}}$  are the corresponding amplitudes.

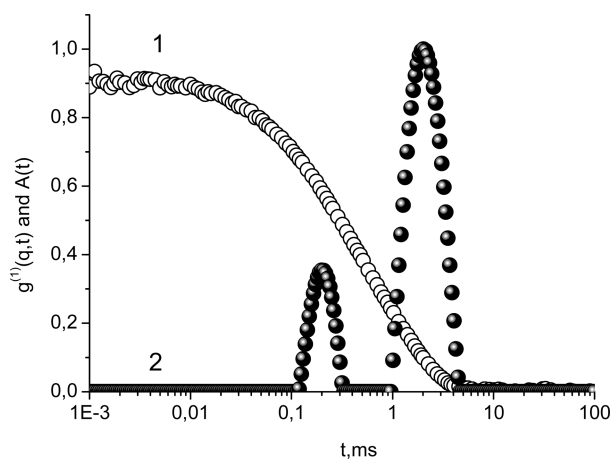


**Figure 1.** Semilog representation of the field autocorrelation function,  $g^{(1)}(q,t)$  (1), and the distribution function of the decay time,  $A(t)$  (2), for a 0.7 g/L aqueous solution of HM chitosan HMC-2% containing 0.3 M  $\text{CH}_3\text{COOH}/0.1$  M NaCl at scattering angle  $\theta = 90^\circ$ .

Both modes were shown to be due to the translational diffusion of particles, as the relaxation rates,  $\Gamma$ , being plotted as a function of the square of the scattering vector,  $q^2$ , yielded straight lines passing through the origin (Figure 2). As was demonstrated previously,<sup>11</sup> the fast mode can be attributed to individual macromolecules (or unimers), whereas the slow mode providing the main input in the scattering intensity corresponds to multichain aggregates.

The apparent diffusion coefficients,  $D_{\text{app}}$ , of the particles estimated from the slope of  $\Gamma(q^2)$  plots were extrapolated to zero polymer concentration. From the obtained values of the diffusion coefficients,  $D$ , at infinite dilution, the hydrodynamic radii of the particles were calculated using the Einstein–Stokes equation (eq 6). The results obtained are summarized in Table 4. It is seen that the hydrodynamic radii of the unimers do not change with increasing amount of hydrophobic groups in the polymer and are equal to those of the unmodified chitosan sample, which indicates the absence of intramolecular aggregation, which is consistent with the viscosity data.

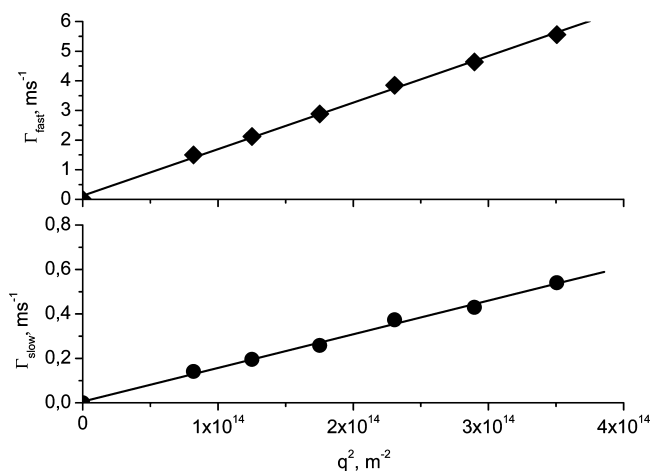


**Figure 2.** Relaxation rate as a function of the square of the scattering vector,  $q^2$ , for fast (top) and slow (bottom) modes for a 0.7 g/L aqueous solution of HM chitosan HMC-2% containing 0.3 M  $\text{CH}_3\text{COOH}/0.1$  M NaCl.

**Table 4.** Radii of Unimers and Aggregates in Dilute Aqueous Solutions of Chitosan and HM Chitosan in 0.3 M  $\text{CH}_3\text{COOH}$  at Different Concentrations of NaCl

[NaCl], M	DS, mol %	$R_{\text{H,univ}}^a$ , nm	$R_{\text{H,agg}}^a$ , nm	$R_{\text{g,agg}}$ , nm	$(R_{\text{g}}/R_{\text{H}})_{\text{agg}}$
0.025	0	$25 \pm 2$	$160 \pm 5$	$62 \pm 2$	0.39
	2	$24 \pm 2$	$158 \pm 5$	$72 \pm 1$	0.44
	4	$24 \pm 2$	$160 \pm 5$	$75 \pm 2$	0.47
0.05	0	$19 \pm 1$	$138 \pm 5$	$62 \pm 2$	0.45
	2	$19 \pm 1$	$134 \pm 5$	$71 \pm 1$	0.53
	4	$19 \pm 1$	$134 \pm 5$	$72 \pm 2$	0.54
0.1	2	$15 \pm 1$	$104 \pm 2$	$69 \pm 2$	0.66
	4	$15 \pm 1$	$106 \pm 3$	$70 \pm 2$	0.66

<sup>a</sup>The values are extrapolated to zero concentration of polymer.

Table 4 shows that the hydrodynamic radii of the aggregates,  $R_{\text{H,agg}}$ , are also independent of the content of the hydrophobic units in chitosan. To explain this observation, it is important to analyze the effect of hydrophobic substituents on the radii of gyration,  $R_{\text{g,agg}}$ , and on the molecular weight of the aggregates,  $M_{\text{agg}}$ , which will be done hereafter.

The radii of gyration of the aggregates,  $R_{\text{g,agg}}$ , were obtained from the scattering intensity provided by the slow mode using eq 7. We suggest that this approach gives more reliable data than the extraction of  $R_{\text{g,agg}}$  from the apparent radius of gyration,  $R_{\text{g}}^*$ , determined from Zimm plots.<sup>11</sup> From Table 4 it is seen that the radii of gyration of the aggregates,  $R_{\text{g,agg}}$ , increase with increasing content of hydrophobic groups in the polymer. This is in contrast to the behavior of the hydrodynamic radii,  $R_{\text{H,agg}}$ , which stay constant with enhancement of the polymer hydrophobicity (Table 4). The values of  $(R_{\text{g}}/R_{\text{H}})_{\text{agg}}$  of the aggregates lie in the range 0.39–0.66 (Table 4), which is even lower than for the hard sphere (0.778<sup>41,42</sup>). As was demonstrated previously,<sup>11</sup> such low values of the ratio  $(R_{\text{g}}/R_{\text{H}})_{\text{agg}}$  may indicate that the scattering objects represent nanogels, which have a shell with much lower density than the core and therefore a much larger hydrodynamic radius in comparison with the radius of gyration. The core–shell structure may appear as a result of the self-organization of polymer chains inside the aggregate in such a way that more hydrophobic fragments enriched in associating groups are localized in the core whereas hydrophilic fragments reside in

the shell. In particular, one can expect the formation of many dangling chains on the surface of nanogels. Indeed, the macromolecules of HM chitosan with a low content of hydrophobic grafts should have rather long chain ends free of hydrophobes. Most of these ends should be repelled from the aggregate, because they do not carry any attractive sites; moreover, they possess many repulsive sites trying to escape the similarly charged aggregate. Analogous behavior is expected for long hydrophilic fragments in the inner part of the polymer chain; in this case loops in the shell will be formed.

In the core–shell aggregates the highly swollen shell only slightly affects  $R_{g,agg}$ , whereas it contributes significantly to  $R_{H,agg}$ . The fact that the  $R_{g,agg}$  value increases with increasing polymer hydrophobicity means that the core grows. At the same time,  $R_{H,agg}$  remains unchanged; that is, the growth of the core is accompanied by the thinning of the swollen shell. This obviously results from the fact that polymer chains with a higher content of hydrophobic substituents possess longer hydrophobic fragments forming the core and shorter hydrophilic fragments composing the shell.

To determine the molecular weight of the aggregates,  $M_{agg}$ , a combination of DLS and SLS techniques was employed. Figure 3 shows the Zimm plots for the solutions of the HM chitosan

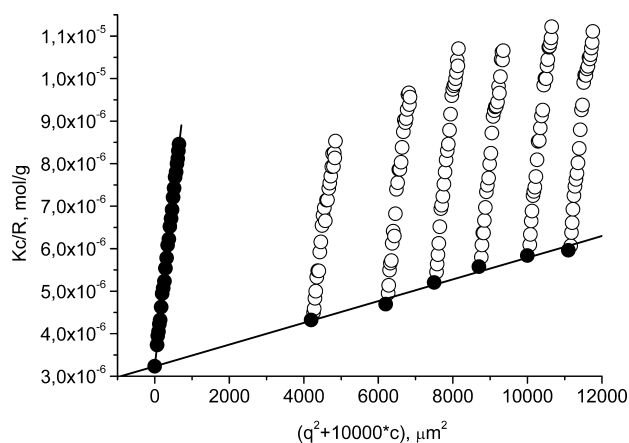


**Figure 3.** Zimm plot for aqueous solutions of HM chitosan HMC-2% in a range of concentrations of 0.25–0.9 g/L in 0.3 M  $\text{CH}_3\text{COOH}/0.025$  M NaCl.

sample. It is seen that the angular dependences of the scattering are essentially linear in the angular range  $35\text{--}150^\circ$ . The absence of curvature whatever the concentration of the polymer evidences that the aggregates are not concentration dependent, which suggests a type of “closed” phenomenon of macromolecular association.<sup>43</sup>

From the Zimm plots the values of the apparent weight-average molecular weight,  $M_w^*$ , the apparent z-average radius of gyration,  $R_g^*$ , and the second virial coefficient,  $A_2$ , were determined. They are collected in Table 5. It is seen that with increasing content of hydrophobic units in the polymer the values of  $A_2$  decrease, i.e., the quality of the solvent becomes poorer. Simultaneously, the apparent weight-average molecular weight,  $M_w^*$ , gets bigger, indicating that enhancement of the polymer hydrophobicity promotes aggregation. It should be noted that the values of  $M_w^*$  contain the contributions of both unimers and aggregates:<sup>44,45</sup>

$$M_w^* = (1 - x_{agg})M_{uni} + x_{agg}M_{agg} \quad (11)$$

**Table 5.** Apparent Weight-Average Molecular Weight,  $M_w^*$ , Apparent z-Average Radius of Gyration,  $R_g^*$ , and Second Virial Coefficient,  $A_2$ , Determined from Zimm Plots for Dilute Aqueous Solutions of Chitosan and HM Chitosan in 0.3 M  $\text{CH}_3\text{COOH}$  at Different Concentrations of NaCl

[NaCl], M	DS, mol %	$M_w^*$	$R_g^*$ , nm	$A_2 \times 10^4$ , ( $\text{cm}^3 \text{mol}/\text{g}^2$ )
0.025	0	145 000	62	12
	2	310 000	72	10
	4	530 000	77	7.0
0.05	0	190 000	62	10
	2	540 000	70	2.1
	4	700 000	75	1.6
0.1	2	550 000	69	1.4
	4	870 000	70	1.3

where  $M_{uni}$  and  $M_{agg}$  are the weight-average molecular weights of unimers and aggregates, respectively, and  $x_{agg}$  is the weight fraction of the aggregates.

Therefore, the observed increase of  $M_w^*$  can be due both to a higher fraction of aggregated chains,  $x_{agg}$ , and/or to a larger molecular weight of aggregates,  $M_{agg}$ . To understand which of these contributions is more important, the values of  $x_{agg}$  and  $M_{agg}$  were estimated separately.

Below we describe the approach which was used for this purpose. First, it was important to determine the correct value of the weight-average molecular weight of unimers,  $M_{uni}$ , which is not always easy for polymers demonstrating a strong tendency toward aggregation. Here, the  $M_{uni}$  values were estimated by SLS at the conditions when the aggregation is suppressed. These conditions include the use of 0.3 M  $\text{CH}_3\text{COOH}/0.2$  M  $\text{CH}_3\text{COONH}_4$  as a solvent breaking the interchain hydrogen bonds in chitosan solutions<sup>5,46,47</sup> and filtration through a filter with a pore size of 0.45  $\mu\text{m}$ . By ninhydrin reaction,<sup>31–33</sup> no loss of polymer on the filter was observed. Figure 4 shows that DLS measurements do not detect any aggregates just after the filtration, but then they reform with time. The kinetics of the re-formation of aggregates after their disruption at filtration was followed at two angles,  $\theta = 90^\circ$  and  $\theta = 40^\circ$ , taking into account that at a lower angle the contribution of big particles is more pronounced. From Figure 4 it is seen that the aggregates begin to reappear only approximately 2 h after filtration, which gives enough time to perform all SLS measurements necessary for the determination of the molecular weight of the unimers. In this way the molecular weight of nonaggregated chains,  $M_{uni}$ , was determined. It equals 75 000.

Once the molecular weight of nonaggregated macromolecules was determined, the next step consisted in the determination of the ratio of the amplitudes of slow and fast modes,  $A_{slow}/A_{fast}$ , of the electric field autocorrelation function from the DLS data. This ratio is related to the values of  $x_{agg}$  and  $M_{agg}$  through the following equation:

$$\frac{A_{slow}}{A_{fast}} = \frac{x_{agg}M_{agg}}{(1 - x_{agg})M_{uni}} \quad (12)$$

Finally, by solving a system of two linear equations (eqs 11 and 12) the values of  $M_{agg}$  and  $x_{agg}$  were deduced. On the basis of the values of  $M_{agg}$ , the aggregation numbers,  $N_{agg}$ , were calculated as  $M_{agg}/M_{uni}$ . The values of  $x_{agg}$ ,  $M_{agg}$ , and  $N_{agg}$  thus obtained are presented in Table 6.

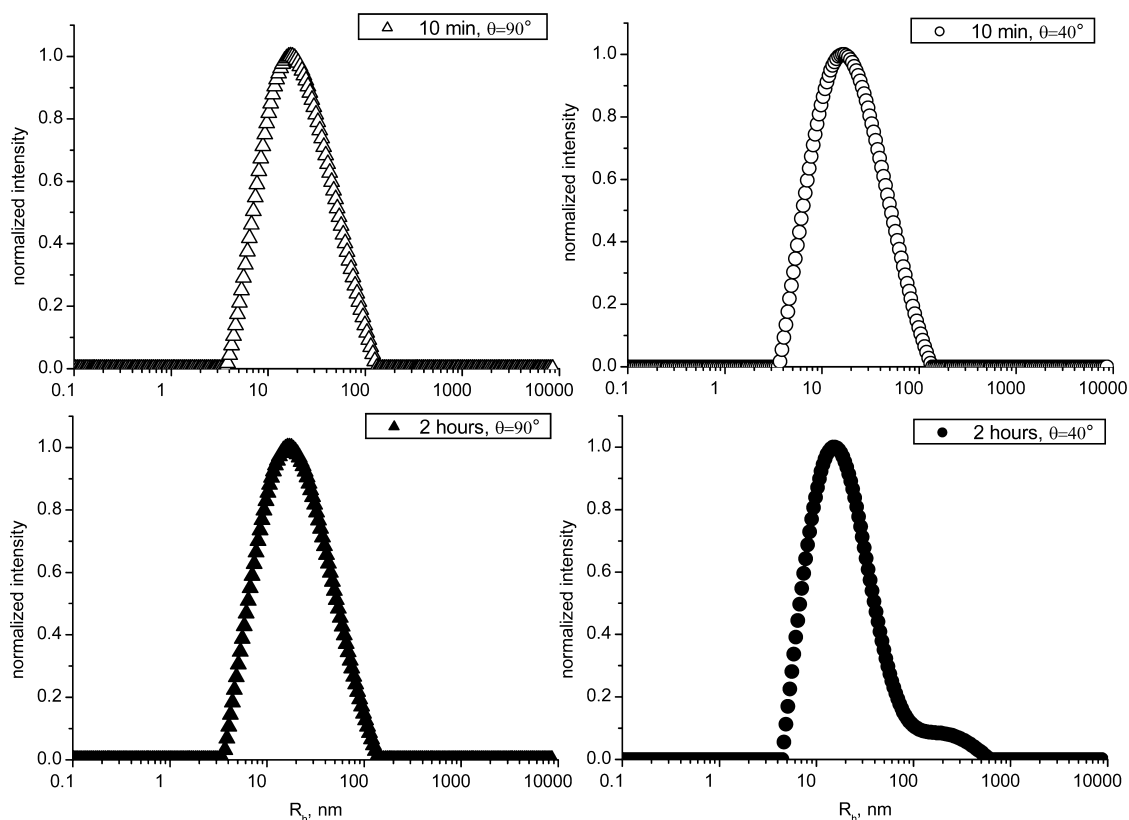


**Figure 4.** Hydrodynamic radius distributions in dilute aqueous solutions of chitosan containing 0.3 M  $\text{CH}_3\text{COOH}/0.2$  M  $\text{CH}_3\text{COONH}_4$  at scattering angles  $\theta = 90^\circ$  and  $\theta = 40^\circ$  10 min and 2 h after filtration through a  $0.45 \mu\text{m}$  filter.

**Table 6. Weight Fraction of the Aggregates,  $x_{\text{agg}}$ , Their Molecular Weight,  $M_{\text{agg}}$ , Aggregation Numbers,  $N_{\text{agg}}$ , and Polymer Volume Fraction inside the Aggregates,  $\phi_{\text{g,agg}}$ , for Dilute Aqueous Solutions of Chitosan and HM Chitosan in 0.3 M  $\text{CH}_3\text{COOH}$  at Different Concentrations of NaCl**

[NaCl], M	DS, mol %	$x_{\text{agg}}$	$M_{\text{agg}}$	$N_{\text{agg}}$	$\phi_{\text{g,agg}} \times 10^4$
0.025	0	0.10	750 000	$10 \pm 1$	$7.1 \pm 0.8$
	2	0.17	1 400 000	$19 \pm 2$	$8.5 \pm 0.8$
	4	0.33	1 500 000	$20 \pm 2$	$8.4 \pm 0.8$
0.05	0	0.16	825 000	$11 \pm 1$	$7.8 \pm 0.8$
	2	0.31	1 400 000	$19 \pm 3$	$9.0 \pm 0.9$
	4	0.38	1 500 000	$20 \pm 3$	$9.2 \pm 0.9$
0.1	2	0.36	1 350 000	$18 \pm 2$	$9.4 \pm 0.9$
	4	0.63	1 400 000	$19 \pm 2$	$9.5 \pm 0.9$

It is seen that with increasing polymer hydrophobicity the fraction of aggregated chains,  $x_{\text{agg}}$ , grows, which manifests enhancement of aggregation as a result of the additional contribution of hydrophobic interactions to the association energy. At the same time, the behavior of the aggregation numbers,  $N_{\text{agg}}$ , is more complicated (Table 6). Let us first compare the  $N_{\text{agg}}$  values for unmodified and HM chitosan. From Table 6 it is seen that the incorporation of hydrophobic units into chitosan chains leads to 2-fold growth of the aggregation numbers,  $N_{\text{agg}}$ . This is obviously due to enhancement of intermolecular aggregation as a result of hydrophobic interactions between *n*-alkyl side groups. It is important to note that despite the 2-fold increase in the aggregation numbers the gyration radii of the aggregates increase only slightly when passing from chitosan to HM chitosan (Table 3). Therefore, the aggregates of HM chitosan are denser (Table 6), which may

be due to the presence of additional cross-links formed by associating *n*-alkyl side groups.

Now let us compare the data for HM chitosan with different amounts of hydrophobic substituents. From Table 6 it is seen that with an increase of the content of *n*-dodecyl groups from 2 to 4 mol % the aggregation number,  $N_{\text{agg}}$ , remains constant despite a rather pronounced growth of the fraction of aggregated chains,  $x_{\text{agg}}$ . Probably, already the introduction of 2 mol % hydrophobic substituents has led to reconstruction of the aggregates, allowing the simultaneous formation of two types of cross-links inside the core: (1) those inherent to chitosan<sup>8</sup> and (2) micelle-like domains composed of *n*-dodecyl side groups. A further increase of the aggregation number may be unfavorable because of pronounced steric hindrances hampering the proper mutual arrangement of polymer chains to realize the maximum possible amount of links between them.

It should be pointed out that the independence of the aggregation number on the DS has already been shown for uncharged HM pullulans,<sup>48</sup> but in that case the aggregates were rather dense. Here we demonstrate that similar behavior can be observed for a charged HM polysaccharide forming highly swollen aggregates with a polymer weight fraction of only  $10^{-3}$  (Table 6). Note that the aggregates are stable for weeks, showing no important change in the size or size distribution or the solution scattered light intensity.

Thus, the increase of the content of hydrophobic units from 2 to 4 mol % induces an increase of the amount of aggregates, but does not affect their aggregation numbers. Simultaneously, within the aggregates, the dense core grows and the swollen shell shrinks, while the hydrodynamic radii remain unchanged.

**Effect of the Salt Concentration.** As the self-aggregation of HM chitosan proceeds between similarly charged macromolecules, it should depend significantly on electrostatic interactions. These interactions induce the repulsion between aggregating chains. Also, they lead to entrapment of some counterions within macromolecules or their aggregates to lower their Coulomb energy. As the self-aggregates trap more counterions<sup>17,18</sup> than the single chains, from which they are composed, the entropy of the system decreases upon aggregation. The role of both these factors (electrostatic repulsion and loss of translational entropy of counterions) counteracting the self-assembly can be reduced by added salt, so salt is expected to favor aggregation of HM chitosan.

In this study, NaCl was chosen as a low molecular weight salt because it does not influence the pH value of the medium in contrast to widely used sodium acetate. It is known<sup>49,50</sup> that salt can affect appreciably the properties of a polyelectrolyte only if its concentration is comparable to that of the counterions. For this reason the NaCl concentrations used were much higher (0.025–0.1 M) than the maximum estimated concentration of chitosan counterions inside the single coils (or aggregates), 0.01 M. On the other hand, these concentrations of NaCl were insufficient to screen completely the electrostatic interactions as is evident from the large values of the Debye screening lengths,  $r_D$  (Table 1), far exceeding the average distance between the charged units in the polymer chains.

Let us first consider the effect of NaCl on the viscosity of dilute solutions of HM chitosan. The results are presented in Table 3. It is seen that salt reduces the intrinsic viscosity, indicating compaction of individual coils. This observation is in full agreement with the DLS data, which demonstrate that the hydrodynamic radii of the unimers,  $R_{H,uni}$ , become smaller with increasing salt concentration (Table 4). The fact that the intrinsic viscosity and the hydrodynamic radii of the unimers,  $R_{H,uni}$ , are independent of the hydrophobicity of the polymer (Tables 3 and 4) testifies that the hydrophobic interactions are not responsible for the compaction. The shrinking proceeds because salt ions penetrate inside the coils and screen the electrostatic repulsion inside them. Also, due to the Donnan effect<sup>18,51</sup> the concentration of salt ions in the outer solution remains higher than inside the macromolecules, which reduces the osmotic pressure of the counterions, thus further compressing the coils.<sup>52</sup> Therefore, shrinking of macromolecules in salt solutions should be due mainly to two effects: screening of electrostatic repulsion between similarly charged units and a decrease of the osmotic pressure exerted by the counterions located inside the polymer coils.

Table 3 shows that at the addition of salt the Huggins constants,  $k_{HV}$ , become higher, pointing to stronger interactions between macromolecules. At the same time, the DLS data (Table 6) evidence that with increasing salt concentration the fraction of aggregates increases (and simultaneously the contribution of unimers to the scattering intensity becomes lower as is seen from Figure 5). Thus, salt promotes aggregation between similarly charged macromolecules as expected.

The most interesting is the behavior of the aggregation numbers. Table 6 shows that they are absolutely independent of the amount of added salt. This result is quite unexpected as we are dealing with charged aggregates. Indeed, one could suggest that screening of the electrostatic repulsion will allow to more similarly charged polyelectrolyte chains to be accommodated within one aggregate. The fact that, in the present

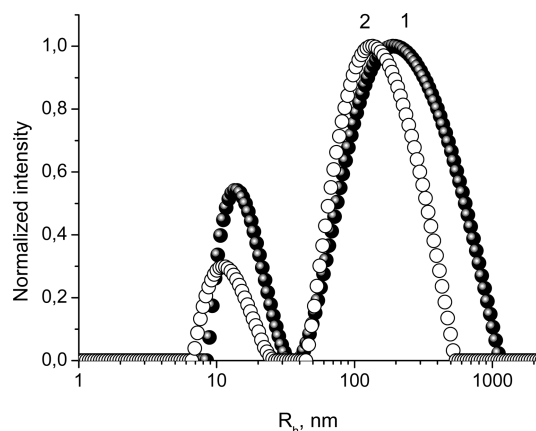


**Figure 5.** Hydrodynamic radius distributions in a 0.5 g/L solution of HM chitosan HMC-2% in 0.3 M  $\text{CH}_3\text{COOH}$  containing different amounts of NaCl: 0.025 M (1) and 0.05 M (2).

system, the aggregation numbers remain unchanged may be due to the core–shell structure of the aggregates, in which a hydrophilic shell poor in associating groups provides a quite low surface energy, making growth of the aggregates unfavorable. The independence of the aggregation numbers of charged core–shell aggregates on the amount of added salt was previously observed for some diblock<sup>53</sup> and multiblock<sup>54</sup> copolymer micelles with a core composed of neutral blocks and corona formed by polyelectrolyte blocks. The absence of a salt effect on the self-assembly behavior of the diblock copolymers was explained by the glassy state of their micellar core. In such a case, the aggregation numbers are governed by the requirement to pack closely the neutral block chains within the core, and therefore, they are determined mainly by the core block properties, in particular its length.<sup>53</sup> In the present study we first demonstrate that the independence of the aggregation number on the amount of added salt can also be observed for random copolymer aggregates with charged units both in the core and in the shell. One can suggest that in this case the independence of  $N_{agg}$  on the salt concentration may also result from rather strong attraction between the associating groups in the core despite the fact that the core is not densely packed and contains an enormous amount of solvent. Such a strong attraction may be due, for example, to the crystallization of some junction zones between chitosan chains. The possibility of formation of crystallites in chitosan aggregates was recently demonstrated for several samples of unmodified chitosan.<sup>14,15</sup> In this case the aggregation number will depend on the possibility to realize the maximum possible amount of intermolecular links per chain in the core. When the aggregation number is lower, a small content of associating groups does not permit a sufficient gain in association energy. On the other hand, at too high  $N_{agg}$  some of the links cannot be formed because of steric hindrances. Thus, it seems that the aggregation number depends primarily on the optimum packing of the chains within the core to get the highest gain in the association energy. In its turn, the role of the shell consists in the stabilization of the aggregates due to a combination of electrostatic repulsion (dominating at low salt content) and steric interactions (prevailing at higher salt content).

One could think that the  $N_{agg}$  values in HM chitosan are so stable because the aggregates represent frozen structures (such as the glassy core in the above-mentioned diblock copolymers),

but this is not the case as the aggregation numbers are highly sensitive to some other factors such as the length of single macromolecules<sup>11</sup> and the type of added salt.<sup>12,55</sup> Also, they are in dynamic equilibrium with individual macromolecules as their fraction increases at dilution (Figure 6). In addition, it should

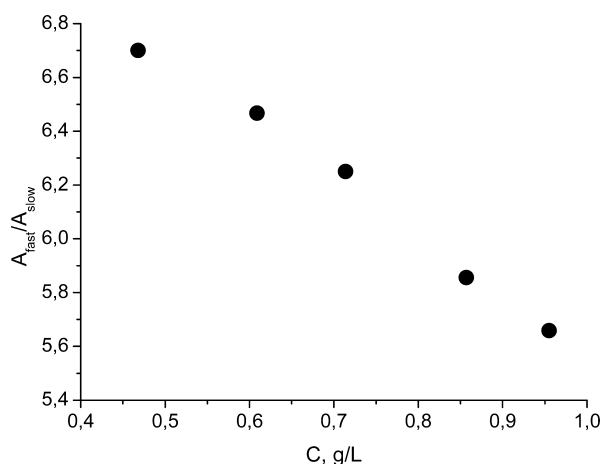


**Figure 6.** Dependence of the ratio of the amplitude of fast and slow modes,  $A_{\text{fast}}/A_{\text{slow}}$  of the electric field autocorrelation function on the concentration of HM chitosan HMC-2% in aqueous solution containing 0.3 M acetic acid/0.05 M sodium chloride at a scattering angle of 90°.

be pointed out that the characteristics of the aggregates are independent of the procedure of their preparation: by direct dissolution of HM chitosan in acidic aqueous salt solution or by adding salt to the acidic aqueous solution of polymer.

Now let us consider the radii of the aggregates. From Table 4 it is seen that both  $R_{\text{H,agg}}$  and  $R_{\text{g,agg}}$  decrease upon addition of salt. This is due to screening of the electrostatic repulsion and lowering of the osmotic pressure exerted by counterions trapped by the aggregates. One more reason may consist in the fact that salt promotes the formation of additional hydrophobic domains linking different polymeric chains within the aggregates. To check this suggestion, we studied the ability of the aggregates to absorb pyrene molecules poorly soluble in water: the greater the total volume of hydrophobic domains, the larger the amount of pyrene solubilized in their interior. Figure 7 shows that the limiting concentration of pyrene in HM chitosan solution becomes higher with increasing salt content. The effect observed cannot be explained only by the larger amount of aggregates. Indeed, when the NaCl concentration changes from 0.025 to 0.1 M, the fraction of aggregated chains demonstrates a 2-fold growth (Table 6), whereas the maximum amount of solubilized pyrene increases by a factor of 3 (Figure 7). Therefore, salt increases not only the number of aggregates, but also the total volume of hydrophobic domains inside them.

To gain insight into the effect of salt on the structure of aggregates of HM chitosan, the values of the ratio  $(R_{\text{g}}/R_{\text{H}})_{\text{agg}}$  were analyzed. From Table 4 it is seen that with increasing salt concentration the ratio  $(R_{\text{g}}/R_{\text{H}})_{\text{agg}}$  becomes higher, approaching the value of the homogeneous hard sphere; i.e., the shell of the nanogels with lower density shrinks considerably much more than the core. Simultaneously, the polymer volume fraction,  $\varphi_{\text{agg}}$  inside the aggregates slightly grows (Table 6). Nevertheless, it should be noted that the values of  $\varphi_{\text{agg}}$  remain rather low; that is, the nanogels retain their highly swollen state. This may be explained by a pronounced rigidity of the

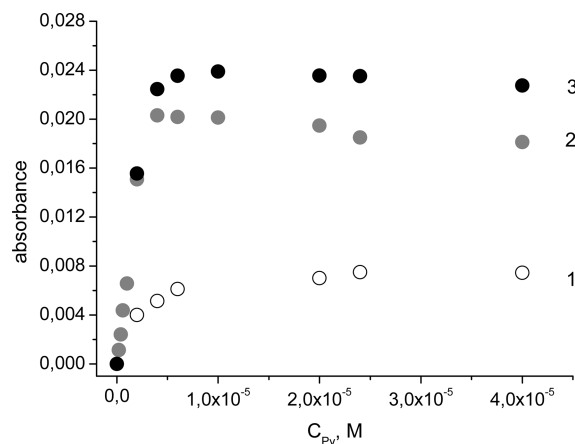


**Figure 7.** Absorbance at 338 nm as a function of the concentration of pyrene added to a 1 g/L aqueous solution of HM chitosan HMC-4% in 0.3 M  $\text{CH}_3\text{COOH}$  at different NaCl concentrations: 0.025 M (1), 0.05 M (2), and 0.1 M (3) (the absorbance is measured relative to the absorbance of unmodified chitosan solutions containing pyrene prepared at the same conditions).

polymeric network in the core, which counteracts its shrinking. The fact that the inner core of aggregates of HM chitosan can be rigid was demonstrated<sup>21</sup> recently by the measurements of the rotational motion of the 1,6-diphenyl-1,3,5-hexatriene probe, giving large anisotropy values exceeding those for aggregates of, e.g., poly(1-octadecene-co-maleic acid). One can suggest that the rigidity of the core may arise from the semirigid character of chitosan chains<sup>2</sup> and multiple crystallites acting as the junction zones between them.

Thus, increasing the salt concentration produces almost the same effect on the aggregation of HM chitosan as the growing content of hydrophobic units (2–4 mol %): it augments the fraction of aggregated macromolecules while keeping the aggregation numbers constant. The difference concerns their effects on the size of the aggregates: salt induces contraction of the whole aggregates (both  $R_{\text{H,agg}}$  and  $R_{\text{g,agg}}$  decrease), whereas increasing DS leads to some expansion of the core of the aggregates ( $R_{\text{g,agg}}$  increases) at the expense of their highly swollen shell resulting in a constant  $R_{\text{H,agg}}$  value.

## CONCLUSIONS

In dilute aqueous solutions, both chitosan and HM chitosan demonstrate the ability to self-assemble into core–shell aggregates with hydrophobic fragments in the core and hydrophilic ones in the shell. It was shown that introducing hydrophobic groups into the chitosan chain and increasing the salt concentration promotes the aggregation as in both cases the weight fraction of the aggregates increases.

The most striking observation is that the aggregates are formed from a roughly constant number of chains regardless of the amount of associating groups (2 or 4 mol %) or of the added salt (0.025–0.1 M). Probably, this optimum number of chains permits the realization of a maximum amount of intermolecular links per chain inside the core.

Such stable aggregates are attractive as delivery carriers for poorly water-soluble drugs which can be solubilized in their hydrophobic domains. In addition, these aggregates are expected to incorporate water-soluble, polar or anionic substrates, such as peptides, proteins, and polynucleotides,

which can interact with chitosan by hydrogen bonds or electrostatic interactions.<sup>3</sup>

## AUTHOR INFORMATION

### Corresponding Author

\*E-mail: phil@polly.phys.msu.ru.

### Notes

The authors declare no competing financial interest.

## ACKNOWLEDGMENTS

The financial support of the program Scientific and Educational Staff of Innovative Russia in 2009–2013 is gratefully acknowledged. We express our gratitude to Prof. A. R. Khokhlov, Prof. I. I. Potemkin, Dr. V. O. Aseyev, and Dr. I. V. Blagodatskikh for many fruitful discussions.

## REFERENCES

- (1) Aranz, L.; Harris, R.; Heras, A. *Curr. Org. Chem.* **2010**, *14*, 308–330.
- (2) Rinaudo, M. *Prog. Polym. Sci.* **2006**, *31*, 603–632.
- (3) Uragami, T.; Tokura, S. *Material Science of Chitin and Chitosan*; Springer, Kodansha Ltd.: Tokyo, 2006.
- (4) Rinaudo, M.; Milas, M.; Le Dung, P. *Int. J. Biol. Macromol.* **1993**, *15*, 281–285.
- (5) Anthonsen, M. W.; Vårum, K. M.; Hermansson, A. M.; Smidsrød, O.; Brant, D. A. *Carbohydr. Polym.* **1994**, *25*, 13–23.
- (6) Amiji, M. M. *Carbohydr. Polym.* **1995**, *26*, 211–213.
- (7) Ottøy, M. H.; Vårum, K. M.; Christensen, B. E.; Anthonsen, M. W.; Smidsrød, O. *Carbohydr. Polym.* **1996**, *31*, 253–261.
- (8) Philippova, O. E.; Volkov, E. V.; Sitnikova, N. L.; Khokhlov, A. R.; Desbrières, J.; Rinaudo, M. *Biomacromolecules* **2001**, *2*, 483–490.
- (9) Sorlier, P.; Rochas, C.; Morfin, I.; Viton, C.; Domard, A. *Biomacromolecules* **2003**, *4*, 1034–1040.
- (10) Popa-Nita, S.; Alcouffe, P.; Rochas, C.; David, L.; Domard, A. *Biomacromolecules* **2010**, *11*, 6–12.
- (11) Korchagina, E. V.; Philippova, O. E. *Biomacromolecules* **2010**, *11*, 3457–3466.
- (12) Philippova, O. E.; Korchagina, E. V. *Polym. Sci., Ser. C* **2012**, in press.
- (13) Aiba, S. *Int. J. Biol. Macromol.* **1991**, *13*, 40–44.
- (14) Philippova, O. E.; Korchagina, E. V.; Volkov, E. V.; Smirnov, V. A.; Khokhlov, A. R.; Rinaudo, M. *Carbohydr. Polym.* **2012**, *87*, 687–694.
- (15) Brunel, F.; Véron, L.; Ladavière, C.; David, L.; Domard, A.; Delair, T. *Langmuir* **2009**, *25*, 8935–8943.
- (16) Sogias, I. A.; Khutoryanskiy, V. V.; Williams, A. C. *Macromol. Chem. Phys.* **2010**, *211*, 426–433.
- (17) Potemkin, I. I.; Vasilevskaya, V. V.; Khokhlov, A. R. *J. Chem. Phys.* **1999**, *111*, 2809–2817.
- (18) Potemkin, I. I.; Andreenko, S. A.; Khokhlov, A. R. *J. Chem. Phys.* **2001**, *115*, 4862–4872.
- (19) Zhang, C.; Ding, Y.; Ping, Q.; Yu, L. *J. Agric. Food Chem.* **2006**, *54*, 8409–8416.
- (20) Lee, K. Y.; Jo, W. H.; Kwon, I. C.; Kim, Y.-H.; Jeong, S. Y. *Langmuir* **1998**, *14*, 2329–2332.
- (21) Lee, K. Y.; Jo, W. H.; Kwon, I. C.; Kim, Y.-H.; Jeong, S. Y. *Macromolecules* **1998**, *31*, 378–383.
- (22) Kwon, S.; Park, J. H.; Chung, H.; Kwon, I. C.; Jeong, S. Y.; Kim, I.-S. *Langmuir* **2003**, *19*, 10188–10193.
- (23) Jiang, G.-B.; Quan, D.; Liao, K.; Wang, H. *Mol. Pharm.* **2005**, *3*, 152–160.
- (24) Jiang, G.-B.; Quan, D.; Liao, K.; Wang, H. *Carbohydr. Polym.* **2006**, *66*, 514–520.
- (25) Li, Y. Y.; Chen, X. G.; Liu, C. S.; Cha, D. S.; Park, H. J.; Lee, C. M. *J. Agric. Food Chem.* **2007**, *55*, 4842–4847.
- (26) Liu, C.-G.; Chen, X.-G.; Park, H.-J. *Carbohydr. Polym.* **2005**, *62*, 293–298.
- (27) Zhu, A.; Dai, S.; Li, L.; Zhao, F. *Colloids Surf., B* **2006**, *47*, 20–28.
- (28) Chen, W. Y.; Hsu, C. H.; Huang, J. C.; Tsai, M. L.; Chen, R. H. *J. Polym. Res.* **2011**, *18*, 1385–1395.
- (29) Rinaudo, M.; Auzely, R.; Vallin, C.; Mullagaliev, I. *Biomacromolecules* **2005**, *6*, 2396–2407.
- (30) Desbrières, J.; Martinez, C.; Rinaudo, M. *Int. J. Biol. Macromol.* **1996**, *19*, 21–28.
- (31) Moore, S.; Stein, W. H. *J. Biol. Chem.* **1948**, *176*, 367–388.
- (32) Moore, S. *J. Biol. Chem.* **1968**, *243*, 6281–6283.
- (33) Prochazkova, S.; Vårum, K. M.; Østgaard, K. *Carbohydr. Polym.* **1999**, *38*, 115–122.
- (34) Rinaudo, M.; Pavlov, G.; Desbrières, J. *Polymer* **1999**, *40*, 7029–7032.
- (35) Grosberg, A. Yu.; Khokhlov, A. R. *Statistical Physics of Macromolecules*; American Institute of Physics Press: New York, 1994.
- (36) Scharlt, W. *Light Scattering from Polymer Solutions and Particles Dispersions*; Springer-Verlag: Berlin, Heidelberg, 2007.
- (37) Zimm, B. H. *J. Chem. Phys.* **1948**, *16*, 1099–1116.
- (38) Provencher, S. W. *Macromol. Chem.* **1979**, *180*, 201–209.
- (39) Huggins, M. J. *Am. Chem. Soc.* **1942**, *64*, 2716–2718.
- (40) Shashkina, Yu. A.; Zaruslov, Yu. D.; Smirnov, V. A.; Philippova, O. E.; Khokhlov, A. R.; Pryakhina, T. A.; Churochkina, N. A. *Polymer* **2003**, *44*, 2289–2293.
- (41) Burchard, W. *Adv. Polym. Sci.* **1999**, *143*, 113–194.
- (42) Aseyev, V. O.; Tenhu, H.; Winnik, F. M. *Adv. Polym. Sci.* **2006**, *196*, 1–85.
- (43) Elias, H.-G. In *Light Scattering from Polymer Solutions*; Huglin, M. B., Ed.; Academic Press: New York, 1972; Chapter 9.
- (44) Zhou, Z.; Peiffer, D. G.; Chu, B. *Macromolecules* **1994**, *27*, 1428–1433.
- (45) Zhang, Y.; Wu, C.; Fang, C.; Zhang, Y.-X. *Macromolecules* **1996**, *29*, 2494–2497.
- (46) Domard, A.; Rinaudo, M. *Polym. Commun.* **1984**, *25*, 55–58.
- (47) Schatz, C.; Viton, C.; Delair, T.; Pichot, C.; Domard, A. *Biomacromolecules* **2003**, *4*, 641–648.
- (48) Akiyoshi, K.; Deguchi, S.; Tajima, H.; Nishikawa, T.; Sunamoto, J. *Macromolecules* **1997**, *30*, 857–861.
- (49) Marko, J. F.; Rabin, Y. *Macromolecules* **1992**, *25*, 1505–1509.
- (50) Jeon, C. H.; Makhaeva, E. E.; Khokhlov, A. R. *Macromol. Chem. Phys.* **1998**, *12*, 2665–2670.
- (51) Potemkin, I. I.; Zeldovich, K. B.; Khokhlov, A. R. *Polym. Sci., Ser. C* **2000**, *42*, 154–171.
- (52) Vasilevskaya, V. V.; Potemkin, I. I.; Khokhlov, A. R. *Langmuir* **1999**, *15*, 7918–7924.
- (53) Dan, N.; Tirrell, M. *Macromolecules* **1993**, *26*, 4310–4315.
- (54) Liu, R. C. W.; Pallier, A.; Brestaz, M.; Pantoustier, N.; Tribet, C. *Macromolecules* **2007**, *40*, 4276–4286.
- (55) Korchagina, E. V.; Philippova, O. E. Manuscript in preparation.